

1 **Mid-Infrared Spectroscopic Analysis of Raw Milk to Predict the Blood Plasma Non-Esterified**
2 **Fatty Acid Concentration in Dairy Cows**

3
4 Ben Aernouts,*†‡1 Ines Adriaens,*† José Diaz-Olivares,*† Wouter Saeys,† Päivi Mäntysaari,§
5 Tuomo Kokkonen,# Terhi Mehtiö,§ Sari Kajava,□ Paula Lidauer,§ Martin H. Lidauer,§ Matti
6 Pastell‡

7
8 *KU Leuven, Department of Biosystems, Biosystems Technology Cluster, Campus Geel,
9 Kleinhoefstraat 4, 2440 Geel, Belgium

10 †KU Leuven, Department of Biosystems, Mechatronics, Biostatistics and Sensors division,
11 Kasteelpark Arenberg 30, 3001 Leuven, Belgium

12 ‡Natural Resources Institute of Finland (Luke), Maarintie 6, 02150 Espoo, Finland

13 §Natural Resources Institute of Finland (Luke), Tietotie 4, 31600 Jokioinen, Finland

14 #University of Helsinki, Department of Agricultural Sciences, Koetilantie 5, 00014 Helsinki,
15 Finland

16 □Natural Resources Institute of Finland (Luke), Halolantie 31 A, 71750 Maaninka, Finland

17
18 ¹Corresponding author: Ben Aernouts, KU Leuven, Department of Biosystems, Biosystems
19 Technology Cluster, Campus Geel, Kleinhoefstraat 4, 2440 Geel, Belgium, +32 (0)14 72 13 64,
20 ben.aernouts@kuleuven.be

21
22 **ABSTRACT**

23 In high yielding dairy cattle, severe postpartum negative energy status is often associated with
24 metabolic and infectious disorders that negatively affect production, fertility and welfare.
25 Mobilization of adipose tissue associated with a negative energy status is reflected through an

26 increased level of non-esterified fatty acids (**NEFA**) in the blood plasma. Earlier, identification of a
27 negative energy status through the detection of increased blood plasma NEFA concentration
28 required laborious and stressful blood sampling. More recently there have been attempts to predict
29 blood NEFA concentration from milk samples. This study aimed to develop and validate a model to
30 predict the blood plasma NEFA concentration using milk mid-infrared (**MIR**) spectra that are
31 routinely measured in the context of milk recording. To this end, blood plasma and milk samples
32 were collected in weeks 2, 3 and 20 post-partum for 192 lactations in 3 different herds. The blood
33 plasma samples were taken in the morning, while representative milk samples were collected during
34 the morning and evening milk session on the same day. To predict the blood plasma NEFA
35 concentration from the milk MIR spectra, partial least squares regression models were trained on
36 part of the observations from the first herd. The models were then thoroughly validated on all other
37 observations of the first herd and on the observations of the two independent herds to explore their
38 robustness and wide applicability. The final model can accurately predict blood plasma NEFA
39 concentrations below 0.6 mmol/L with a root mean square error of prediction (RMSE) of less than
40 0.143 mmol/L. However, for blood plasma with more than 1.2 mmol/L NEFA, the model clearly
41 underestimates the true level. Additionally, it was found that morning blood plasma NEFA levels
42 were predicted with a significantly higher accuracy ($p = 0.009$) using MIR spectra of evening milk
43 samples compared to morning samples, with RMSEP values of respectively 0.182 and 0.197
44 mmol/L and R^2 values of 0.613 and 0.502. These results suggest a time delay between variations in
45 blood plasma NEFA and related milk biomarkers. Based on the MIR spectra of evening milk
46 samples, cows at risk for a negative energy status, indicated with detrimental morning blood plasma
47 NEFA levels (> 0.6 mmol/L), could be identified with a sensitivity and specificity of respectively
48 0.831 and 0.800. As this model can be applied to millions of historical and future milk MIR spectra,
49 it opens opportunities for regular metabolic screening and improved resilience phenotyping.

50 **Key words:** milk mid-infrared spectroscopy, blood plasma non-esterified fatty acid
51 concentration, negative energy status, milk biomarker

52

53

INTRODUCTION

54 The transition from pregnancy to lactation in high-yielding dairy cows is typically accompanied
55 by a negative energy status (**ES**) in which the energy requirement exceeds the energy input from
56 feed. As severe negative ES increases the susceptibility to various health and fertility problems
57 (Leblanc, 2010; Ospina et al., 2010a), the duration and degree of negative ES should be limited
58 through preventive actions in combination with individual monitoring and imperative treatment.

59 To compensate for the energy deficit and maintain high milk production, adipose tissue is
60 mobilized and non-esterified fatty acids (**NEFA**) are released in the blood. Hence, a blood plasma
61 NEFA concentration above 0.6 mmol/L is generally used as an indicator for negative ES in dairy
62 cattle (Ospina et al., 2010b). These high concentrations of circulating NEFA have a detrimental
63 effect on the oocyte quality and the immune response of dairy cows (Leroy et al., 2005; Scalia et al.,
64 2006). In the liver, part of the NEFA are oxidized completely to deliver energy or incompletely to
65 produce ketone bodies (Adewuyi et al., 2005). Another portion of the NEFA is esterified to
66 triglycerides and either stored in the liver or transported as lipoproteins to e.g. the alveolar epithelial
67 cells of the udder tissue to synthesize milk fat. In this way, fatty acids (**FA**) and ketone bodies
68 derived from the NEFA end up in the produced milk. Previous studies have demonstrated the use of
69 milk biomarkers for monitoring negative ES in individual cows, e.g. through the measurement of
70 certain FA (Van Haelst et al., 2008; Jorj Jong et al., 2014; Dórea et al., 2017), ketone bodies
71 (Enjalbert et al., 2010), citrate and many more (Bjerre-Harpøth et al., 2012). In contrast to taking
72 blood samples, milk sampling requires less labor and can be done without distressing the animals.
73 Nevertheless, the reference techniques to measure these milk biomarkers are typically labor-
74 intensive and costly (Jorj Jong et al., 2014).

75 A relatively straightforward and cost-efficient technique for milk analysis is mid-infrared
76 (MIR) spectroscopy. As the covalent bonds of molecules in milk absorb MIR radiation at very
77 specific wavenumbers, the concentrations of these milk components can be derived from the MIR
78 absorbance spectra. Typically, multivariate linear models are trained to predict the milk constituents
79 from the acquired spectra (De Marchi et al., 2014). Already for decades, this technique is accepted
80 as the reference for accurate and routinely characterization of the main milk components in the
81 context of milk recording (ISO, 2013; ICAR, 2019). Since the commercial introduction of Fourier-
82 transform MIR spectrometers for milk analysis, milk MIR spectra can be obtained with a higher
83 accuracy and repeatability. This opens opportunities for measuring minor milk components and
84 milk biomarkers such as FA profiles (Rutten et al., 2009; Afseth et al., 2010; Soyeurt et al., 2011),
85 protein composition (Franzoi et al., 2019), minerals (Soyeurt et al., 2009), ketone bodies and citrate
86 (Grelet et al., 2016).

87 Recently, Benedet et al. (2019), Grelet et al. (2019) and Luke et al. (2019) developed models to
88 predict the blood plasma NEFA concentrations from milk MIR spectra of individual dairy cows.
89 However, the prediction performance of Grelet's model was poor ($R^2 = 0.39$), likely because it was
90 built using a limited number ($n = 234$) of calibration samples (Grelet et al., 2019). Benedet's model
91 performed better ($R^2 = 0.52$), however, like Grelet's model, it was not validated for a completely
92 independent herd (Benedet et al., 2019; Grelet et al., 2019). Accordingly, the reported results might
93 be overoptimistic compared to applying the model on the data of a new herd where the cows are
94 managed differently. This was clearly illustrated by Luke et al. (2019) as the determination
95 coefficient (R^2) of their model dropped from 0.61 for a randomly selected validation set, covering
96 the same herds as the ones included in the calibration set, to 0.45 for a completely independent herd.

97 We hypothesized that a better prediction performance can be obtained through increasing the
98 number of calibration samples and applying a very strict timing in the sampling of blood and milk
99 samples relative to the diurnal pattern and the feeding schedule of the cows (Quiroz-Rocha et al.,

100 2010). To test this hypothesis, a high number of samples was collected following a strict protocol
101 for blood and milk sample collection to obtain high quality data for training the prediction models.
102 Additionally, it is investigated whether MIR spectra of morning or evening milk samples result in a
103 better prediction of the NEFA concentration of the respective blood samples taken in the morning
104 of that day. Finally, the performance of the prediction models is evaluated extensively on a
105 completely independent validation set.

106

107

MATERIALS AND METHODS

108 *Experimental Setup*

109 The experimental protocol was approved by the Finnish Animal Experiment Board
110 (ESAVI/5688/04.10.07/2013) and applied on 3 experimental herds in Finland: Luke Jokioinen (herd
111 A), University of Helsinki in Viikki (herd B) and Luke Kuopio (herd C). All cows in these herds
112 that calved for the first time in the period between September 2013 and October 2016 were included
113 in the study, resulting in a total of 143 Nordic Red dairy cows from which 103 were in herd A, 24 in
114 herd B and 16 in herd C. For 49 of these 143 cows, also the second lactation was included in the
115 study period, thus resulting in a total of 192 lactations. A detailed description on the housing
116 conditions, ration, feeding frequency and milking conditions and frequency during the experiment is
117 given by Mäntysaari et al. (2019).

118

119 *Data Collection*

120 For each lactation, blood samples were taken from the coccygeal vein within one hour after the
121 morning milking session, on two non-consecutive days in week 2 and in week 3 after calving, and
122 once in week 20. This resulted in a total of 5 blood samples per lactation. Handling of the lactating
123 cows prior to blood-sampling was minimized to reduce its effect on the blood plasma NEFA
124 concentrations (Leroy et al., 2011). Blood was collected in 10 mL EDTA tubes and stored in ice

125 until centrifuged at -4°C for 15 min at $2,000 \times g$. Plasma samples were frozen and stored at -20°C
126 for later analysis of NEFA at the university of Helsinki (Salin et al., 2012). An enzymatic
127 colorimetric acyl-CoA synthetase (ACS)-acyl-CoA oxidase (ACOD) method [NEFA-HR(2) kit,
128 Wako Chemicals GmbH, Neuss, Germany] was used according to the manufacturer's instructions to
129 determine the blood plasma NEFA concentrations, further referred to as 'blood NEFA'. Intra- and
130 interassay coefficient of variation for blood NEFA determination were 1.61 and 3.53% for low
131 NEFA concentration (0.23 mmol/L) and 0.77 and 2.91% for high NEFA concentration (1.24
132 mmol/L).

133 Representative milk samples (± 30 mL) were collected during the morning and evening milking
134 sessions on the same days as the blood collection, providing a total of 10 milk samples per lactation.
135 The milk samples were stored at 4°C using a preservative (± 0.3 mg bronopol per ml milk, Broad
136 Spectrum Microtabs II, D and F Control Systems Inc., Dublin, CA). The MIR analyses (MilkoScan
137 FT6000 spectrometer, Foss, Hillerød, Denmark) were carried out by the Valio Ltd. milk laboratory
138 (Seinäjoki, Finland) according to ISO 9622:2013 (ISO, 2013). The MIR spectrum of each milk
139 sample consisted of 1060 values, representing the infrared light transmittance through $50 \mu\text{m}$ of
140 sample between wavenumbers 5010.2 and 925.7 cm^{-1} with a resolution of 4 cm^{-1} . The MIR spectra
141 were standardized following the procedure developed by Grelet et al. (2015). Because of data
142 storage problems, the MIR spectra of 152 morning milk samples and 183 evening milk samples got
143 lost. The resulting final dataset therefore included 808 and 777 MIR spectra for respectively
144 morning and evening milk samples (Table 1).

145

146 ***Prediction of the Blood Plasma NEFA Concentrations from Milk MIR Spectra***

147 The MIR spectra and NEFA concentrations were imported into R version 3.4.3 (R Core Team,
148 2017). Only the spectral regions from 2977 to 2768 cm^{-1} , 1800 to 1684 cm^{-1} and 1607 to 926 cm^{-1}
149 were used in the analysis. Moreover, the signal-to-noise ratio in the spectral regions between 3660

150 and 2977 cm^{-1} , and between 1684 and 1607 cm^{-1} , was considered too low due to substantial MIR
151 absorption by the water molecules. The spectral regions above 3660 cm^{-1} and between 2768 and
152 1800 cm^{-1} were deleted because they do not contain significant spectral information on relevant
153 milk components (Aernouts et al., 2011; Grelet et al., 2019). A principal component analysis
154 (PCA) with maximum 20 principal components was used to identify potential outlier spectra. When
155 both the Q residuals and the Hotelling T^2 statistic were above their 99% confidence limits, the
156 spectrum was removed from the analysis (Bro and Smilde, 2014).

157 As blood samples were only taken once per cow per sampling day, while 2 milk samples were
158 collected for respectively the morning and evening milking session of that day and cow, the number
159 of blood NEFA analyses was half of the amount of milk MIR spectra. Accordingly, the same blood
160 NEFA concentration was assigned to both the morning and the evening milk MIR spectrum of the
161 respective cow and day. The combination of a morning milk MIR spectrum together with the
162 respective blood NEFA concentration is further referred to as a morning observation, while the
163 combination of an evening milk MIR spectrum together with the respective blood NEFA
164 concentration is further referred to as an evening observation. The morning and evening observation
165 of the same cow and day thus have the same blood NEFA concentration, while they have different
166 milk MIR spectra. Next, about 60% of the morning and evening observations of herd A were
167 allocated to the calibration set, while the remaining 40% of the observations of herd A and all
168 observations of herds B and C were assigned to the validation set (Figure 1, step 1). Moreover, the
169 observations of herd A were split 60/40 by applying the duplex selection method after ordering
170 them on their blood NEFA concentration (Snee, 1977). This procedure assured that both sets had
171 similar descriptive statistics. Observations for the same cow were treated as a block with all of them
172 either in the calibration or validation set to prevent overoptimistic validation results in case of
173 modeling cow-specific effects (Kemps et al., 2010).

174 The spectral pre-processing of the MIR spectra was a combination of (1) a logarithmic spectral
175 transformation (Beer, 1852) or not; (2) a baseline correction, detrending, standard normal variates
176 weighting or multiplicative scatter correction (Geladi et al., 1985; Barnes et al., 1989; Ruckstuhl et
177 al., 2001) or none of those; (3) a first or second order Savitzky-Golay derivative with a second order
178 polynomial filter and 10 different spectral window lengths (Savitzky and Golay, 1964) or no
179 derivative and (4) mean centering. This resulted in 210 different combinations, as presented in
180 Figure 1 (step 2) and described in detail in Aernouts et al. (2011). For each of these 210
181 combinations, a partial least squares regression (**PLSR**) model with up to 20 latent variables was
182 built to predict the blood plasma NEFA concentrations, further referred to as ‘predicted blood
183 NEFA’, from the pre-processed MIR spectra (Martens and Næs, 1987). A group-wise cross-
184 validation (**CV**) with 20 groups, each containing spectra of 3 to 4 cows, was performed on the
185 observations of the calibration set to obtain the root mean square error of cross-validation
186 (**RMSECV**). We selected the smallest number of latent variables for which the PLSR model was
187 not significantly worse compared to the same model with the number of latent variables resulting in
188 the lowest RMSECV. The statistical comparison in this procedure was based on a one-sided paired
189 *T*-test ($\alpha = 0.05$) applied on the absolute residuals of the cross-validated observations (Cederkvist et
190 al., 2005). A similar approach was followed to select the best spectral pre-processing combination.
191 Moreover, the PLSR models resulting from the 210 combinations were ranked by increasing
192 RMSECV, and the one with the smallest number of latent variables and not being significantly
193 worse compared to the model with the lowest RMSECV was selected. Again, a one-sided paired *T*-
194 test ($\alpha = 0.05$) on the absolute residuals of the cross-validated observations was used to statistically
195 compare the models (Cederkvist et al., 2005; Aernouts et al., 2011).

196 The selected pre-processing combination was applied on the MIR spectra to be used as an input
197 for 4 different variable selection methods (Figure 1, step 3): variable importance in projection, jack-
198 knife, reversed interval PLSR and forward interval PLSR (Norgaard et al., 2000; Westad and

199 Martens, 2000; Chong and Jun, 2005). Each of these 4 methods resulted in a set of most relevant
200 wavenumbers for which a PLSR model with an optimal number of latent variables was built as
201 described earlier. The performances of these 4 PLSR models were compared mutually and with the
202 model that uses all wavenumbers. Finally, the set of wavenumbers related to the most parsimonious
203 model whose prediction performance was not significantly worse (one-sided paired *T*-test, $\alpha = 0.05$)
204 than that of the model with the lowest RMSECV was selected.

205 The final prediction model (Figure 1, step 4), together with the selected combination of spectral
206 pre-processing techniques and the selected set of wavenumbers, was used to predict the NEFA
207 concentrations of the observations in the validation set. Accordingly, an error or residual could be
208 calculated for each observation of the validation set. Based on these residuals, the root mean square
209 error of prediction (**RMSEP**), further referred to as the ‘prediction error’, was calculated for the
210 entire validation set. Because this validation set is very diverse, containing morning and evening
211 observations from 3 different herds with blood NEFA concentrations ranging from very low to very
212 high, the RMSEP was also calculated for different subsets of the validation set, allowing for a better
213 understanding of the prediction performance of the model under different situations. These subsets
214 were defined based on a combination of the following features:

- 215 • Milking time: only morning observations, only evening observations or both morning and
216 evening observations;
- 217 • Herd: observations from herd A, herd B, herd C or for the 3 herds together;
- 218 • NEFA range: observations with blood NEFA concentrations in the low (0 – 0.6 mmol/L),
219 middle (0.6 – 1.2 mmol/L), high (1.2 – 2.0 mmol/L) or complete range (0 – 2 mmol/L).
220 These ranges were defined like this because 0.6 mmol/L is generally considered as critical
221 threshold (Ospina et al., 2010b) and because the blood NEFA concentration was always
222 underestimated for true concentrations above 1.2 mmol/L.

223 The procedure described above (Figure 1) was initially followed to develop and validate a PLSR
224 model that predicts the blood NEFA independent of the moment of milk sampling by training it on
225 all the observations – both morning and evening – of the calibration set. This model is further
226 referred to as the ‘full model’. To evaluate the effect of restricting the calibration set to only
227 morning or evening observations, 2 new models were trained following the same procedure as
228 elaborated above, but with respectively only the morning or the evening observations of the
229 calibration set for training the respective PLSR models. These models are further referred to as
230 respectively the ‘morning model’ and the ‘evening model’. All 3 models (full, morning and
231 evening) were validated on the same observations – both morning and evening – of the validation
232 set to allow for an objective comparison of the prediction performance.

233 The prediction performances of the 3 models were compared by applying a repeated-measures
234 ANOVA on the absolute residuals for all the observations of the validation set. Moreover, ‘model’
235 was treated as a fixed effect, while ‘sample’ was specified as a random effect in the two-way
236 ANOVA (Cederkvist et al., 2005). When the ANOVA test pointed out a significant effect ($\alpha = 0.05$)
237 of the model, then the performance of the 3 models was compared bilateral using a Tukey HSD
238 multiple comparison ($\alpha = 0.05$). The 3 models were compared for all the observations in the
239 validation set, as well as the observations in the different subsets of the validation set. The model
240 (full, morning or evening) which was not significantly different from the best model for most of the
241 subsets of the validation set was identified as the most robust. This model was further evaluated on
242 its ability to identify detrimental blood plasma NEFA concentrations (next section). Finally, a 4-
243 way ANOVA analysis, with the model, the milking time, the herd, the NEFA range and all possible
244 interactions as fixed factors, was applied on the absolute residuals for the observations of the entire
245 validation set and subsets of the validation set. This analysis was not paired, so the samples could
246 not be taken as a random factor. If one of the interactions was significant ($\alpha = 0.05$) then all possible
247 combinations of the factors involved in these interactions were compared bilateral using the Tukey

248 HSD multiple comparisons. In absence of significant interaction for a factor, the effect of the
249 factors could be interpreted separately. Moreover, if this factor had a significant ($\alpha = 0.05$)
250 influence on the performance, then the different levels within this factor were compared bilateral
251 with the Tukey HSD multiple comparisons.

252

253 ***Identify Detrimental Blood Plasma NEFA Concentrations from Milk MIR Spectra***

254 To evaluate whether the predicted blood NEFA concentrations can be used to identify
255 detrimental blood NEFA levels (> 0.6 mmol/L), receiver operating characteristic (**ROC**) analyses
256 were performed (Ospina et al., 2010b; Jorjong et al., 2014; Dórea et al., 2017). The ROC curves
257 plot the true positive rate or sensitivity versus the true negative rate ($= 1 - \text{specificity}$) for different
258 thresholds applied on the predicted blood NEFA concentration. Only the most robust model, the one
259 that performed best according to the procedure described in the previous section, was subjected to
260 this ROC analysis. A separate analysis was done for the morning and evening observations of the
261 validation set. The R package *pROC* version 1.13.0 (Robin et al., 2011) was used to calculate the
262 ROC curves, to apply binormal smoothing to the ROC curves, to calculate the 95% confidence
263 intervals (**CI**) of sensitivities, specificities and area under the curve (**AUC**) of the smoothed ROC
264 curves and to statistically compare the smoothed ROC curves. The CI were calculated with 100 000
265 bootstrap replicates to obtain a fair estimate of the second significant digit (Fawcett, 2006).
266 Statistical two-sided pairwise comparisons ($\alpha = 0.05$) between ROC were done based on the area
267 under the curve (AUC) and based on the sensitivities at given specificities from 0 to 1 in steps of
268 0.01, both using the bootstrap method with 100,000 replicates.

269

270

RESULTS

271 ***Data Exploration***

272 The MIR transmittance spectra of the 1585 milk samples included in this study are presented in
273 the top part of Figure 2 as the black solid and dotted lines. Lipid absorption peaks can clearly be
274 observed as dips in the MIR transmittance spectra around 2928 & 2858 cm^{-1} , 1745 cm^{-1} , 1455 cm^{-1}
275 and 1157 & 1078 cm^{-1} , corresponding to respectively the C-H (alkyl) stretch, C=O (carbonyl)
276 stretch, C-H bend and C-O stretch vibrations (Fox and McSweeney, 2006; De Marchi et al., 2009).

277 The Hotelling's T^2 and Q -statistics of the PCA model with 7 selected principal components and
278 the scores for the first 2 principal components of that model were far beyond the 99% confidence
279 limits for the spectra of sample 1445 (herd B, evening milking) and sample 1546 (herd C, morning
280 milking), as shown in Appendix A1. Also, the raw transmittance spectra of these 2 outliers,
281 illustrated with black dotted lines in top part of Figure 2, are clearly different from the other 1583
282 spectra, while the corresponding blood NEFA concentrations are not outlying. This suggests that
283 these 2 samples have erroneous spectral measurements and were therefore removed from the
284 dataset.

285 The reliability, accuracy, and robustness of spectroscopic calibrations are restricted to the range
286 of the constituent of interest and the variation in measurement conditions taken into account during
287 the calibration (Williams and Norris, 2001). The descriptive statistics of the blood NEFA
288 concentrations linked to different subsets of milk MIR transmittance spectra are presented in Table
289 2. The entire calibration and validation set contain respectively 790 and 793 observations and they
290 have a very similar mean, standard deviation and range for the blood NEFA. This table also
291 illustrates the larger variability and range of the blood NEFA levels in herd A compared to herd B
292 and C. Likely, this is the result of the higher number of blood samples being collected and analyzed
293 ($n = 658$) and cows being monitored ($n = 103$) in herd A. Additionally, this might also be caused by
294 differences in the genetic background and the management between the herds. The descriptive
295 statistics for morning and evening samples in a same herd(s) are similar, but not exactly the same.

296 This is because for some of the blood plasma samples only the respective morning or evening milk
297 MIR spectra were collected and not both (Table 1).

298

299 *Calibration on MIR Spectra of Morning and Evening Milk Samples (Full Model)*

300 The 790 morning and evening observations of the calibration set were used to build a PLSR
301 model (= full model) that relates the blood NEFA concentrations to the MIR transmittance spectra.
302 The best performance was obtained when the MIR transmittance spectra were pre-processed using a
303 2nd order Savitzky-Golay derivative with a window length of 7 wavenumber variables, followed by
304 mean-centering. After this pre-processing step, the reversed interval PLSR method selected 117
305 wavenumbers that were most informative and resulted in the best model. The most informative
306 regions of the MIR spectra are indicated as the grey regions in Figure 2.

307 Figure 3a shows the RMSECV and the RMSEP as a function of the number of latent variables
308 included in the full PLSR model after applying the best pre-processing and selecting the best
309 wavenumbers. A separate RMSEP is provided for the morning and evening observations of the
310 validation set, respectively indicated with $RMSEP_M$ and $RMSEP_E$. The PLSR model with 6 latent
311 variables, indicated with the green triangle, was finally selected. This model complexity resulted in
312 nearly the minimum $RMSEP_M$ and $RMSEP_E$, confirming the right choice of number of latent
313 variables based on the cross-validation and illustrating the robustness of the full model. Figure 3a
314 clearly shows that the $RMSEP_E$ is smaller than the $RMSEP_M$ and that the latter is smaller than the
315 RMSECV.

316 The regression coefficients for the full model with 6 latent variables are presented with a green
317 solid line in the bottom part of Figure 2. The regression coefficients follow a relatively smooth
318 curve in function of the wavenumbers, which indicates that the PLSR model is not overfitting the
319 calibration data. High absolute values for the regression coefficients were obtained around 2950 cm^{-1}
320 1 , 1750 cm^{-1} and $1150 - 990\text{ cm}^{-1}$, corresponding to important fat absorption bands: respectively the

321 fat B, fat A and C-O stretch vibrations (Afseth et al., 2010). As the PLSR model uses the 2nd
322 derivative of the MIR spectra, some of the peaks in the regression coefficients are located at the
323 flanks rather than the center of typical absorption peaks.

324 Figure 3b presents the predicted versus measured scatter plot for the full model with 6 latent
325 variables. This figure illustrates that the prediction error of the full model varies a lot with the
326 predicted blood NEFA concentration (y-axis), both for the cross-validated observations of the
327 calibration set as well as for the morning and evening observations of the independent validation
328 set. Additionally, the blood NEFA concentration is generally overestimated for true values (x-axis)
329 between 0.2 and 0.55 mmol/L, while it is always underestimated for true concentrations above 1.2
330 mmol/L. The latter could explain why the $RMSEP_M$ and $RMSEP_E$ are lower than the $RMSECV$, as
331 the validation set contains less observations with a very high blood NEFA concentration (Table 2).
332 In Figure 3b, the predictions based on the evening observations of the validation set (blue crosses)
333 are closer to the identity line compared to the ones based on the morning observations of the same
334 set (red circles). This is the reason why the $RMSEP_E$ values are smaller than the $RMSEP_M$ values in
335 Figure 3a and it suggests that the blood NEFA concentration in the morning can be predicted more
336 accurately using MIR spectra of milk samples taken in the evening of that day rather than morning
337 milk samples.

338 The prediction errors of the full model for different subsets of the validation set are
339 summarized in Table 3. The heteroscedastic prediction error of the full model is clearly shown by
340 the increasing $RMSEP$ with increasing blood NEFA range (different horizontal sections of Table 3).
341 Moreover, for the observations in the low blood NEFA range (0 – 0.6 mmol/L), the $RMSEP$ values
342 of the full model are all between 0.062 and 0.143 mmol/L, while for the middle blood NEFA range
343 (0.6 – 1.2 mmol/L), the $RMSEP$ values vary between 0.198 and 0.290 mmol/L. For the high blood
344 NEFA range (1.2 – 2 mmol/L), the $RMSEP$ values of the full model are between 0.620 and 0.793
345 mmol/L. Within the low, middle and high blood NEFA range, the $RMSEP$ values do not differ

346 much between herds, illustrating that the model can be used for new herds as well (cfr. herd B and
347 C). Compared to the morning observations of the validation set, the RMSEP values for evening
348 observations are in most cases slightly higher for the low blood NEFA range, while they are clearly
349 lower for the complete, middle and high blood NEFA ranges. The observations based on the
350 RMSEP values described in this paragraph are similar to the ones based on the RMSECV values
351 obtained from the cross-validation of the calibration samples (results not shown), confirming the
352 robustness of the full model.

353

354 *Calibration on MIR Spectra of Morning or Evening Milk Samples*

355 The PLSR model trained on the morning observations of the calibration set (= morning model),
356 as well as the one trained on the evening observations (= evening model) provided the best results
357 after applying a 2nd order Savitzky-Golay derivative on the MIR transmittance spectra, followed by
358 mean-centering. The optimal window length for the derivative was respectively 7 and 13
359 wavenumber variables. For both models, reversed interval PLSR proved to be the best variable
360 selection method, resulting in respectively 92 and 126 retained wavenumbers (grey regions in
361 Figure 2). Finally, 3 and 5 latent variables were selected for respectively the morning and evening
362 PLSR model. The regression coefficients for the final morning and evening model are presented as
363 respectively the red dashed and blue dotted lines in the bottom part of Figure 2. Both models have
364 high absolute values for the regression coefficients in the regions near important MIR fat absorption
365 bands, similar to the regression coefficients of the full model.

366 Analogues to the RMSEP values of the full model, the prediction errors of the morning and
367 evening model for different subsets of the validation set are also provided in Table 3. The prediction
368 performances of the three models (full, morning and evening) are compared for each subset of the
369 validation set. Within each column (herd x milking time) and a specified blood NEFA range
370 (complete, low, middle or high), RMSEP values with different subscripts indicate significant ($\alpha =$

371 0.05) differences between the 3 models. Most subsets of herd C and some subsets involving herd B
372 indicated no significant difference between the models. For those subsets, it was found that the
373 statistical tests lacked power ($\beta > 0.4$) because of a too low number of samples. Therefore, the
374 further discussion of the model comparison was only based on the tests with sufficient power ($\beta <$
375 0.2), which all happened to indicate a statistical effect of the model. The first column of Table 3
376 presents the RMSEP values for all the observations of the validation set in each of the 4 specified
377 blood NEFA ranges.

378 In the complete range, the full model performs significantly better than the morning and the
379 evening model, while there is no significant difference between the morning and the evening model.
380 The full and evening models are not significantly different for the observations of the validation set
381 in the low blood NEFA range, while they are both significantly better compared to the morning
382 model. On the other hand, for the observations in the middle and high range, the morning model is
383 significantly better than the full model, while the latter is better than the evening model.

384 For the low, middle and high blood NEFA range, the same trends are reflected in the different
385 subsets of the validation set where the observations are split up per herd and/or milking time (Table
386 3, columns 2 to 9). For the complete blood NEFA range, the full model is significantly better
387 compared to the evening model for all validation subsets with only morning observations, while it is
388 significantly better compared to the morning model for all the subsets with evening observations.
389 Additionally, it was found that the blood NEFA concentrations predicted with the morning model
390 were on average 0.042 mmol/L higher compared to the predictions by the full model applied on the
391 same milk MIR spectra, while the evening model resulted in blood NEFA predictions which were
392 on average 0.048 mmol/L lower compared to the predictions by the full model. Given the fact that
393 low blood NEFA concentrations are generally overestimated by the models, while the high blood
394 NEFA concentrations are underestimated (Figure 3b), the morning model results in lower
395 predictions in the high NEFA range, while the evening model results in lower prediction errors for

396 the low NEFA range. This is also clearly reflected by the models' RMSEP values for the different
397 blood NEFA ranges. As the models mainly rely on the absorption by fat-related covalent bonds
398 (Figure 2), the offset between the models probably results from the difference in average fat content
399 between the morning milk samples (4.3%) and the evening milk samples (5.1%) involved in the
400 training. Taken all this into account, it was concluded that the full model is the most robust of the 3
401 models and is therefore further explored in the ROC analysis in the next section.

402 Apart from the comparisons between the full, the morning and the evening model for each of
403 the subsets of the validation set, a single 4-way ANOVA analysis was performed on the residuals of
404 the observations in these different subsets. As all but one of the two-way interactions between the
405 ANOVA factors were significant, the effect of the individual factors could not interpret
406 independently from the other factors involved in the interaction(s). Accordingly, all combinations of
407 the factors involved in these interactions were compared bilateral using a Tukey HSD multiple
408 comparison. This analysis mainly points out that the prediction errors for the middle and high blood
409 NEFA range are significantly higher compared to the complete and low range, but that the absolute
410 levels of these errors depend on the model, the farm and the milking time.

411 Table 3 can also be used to study the difference in prediction error when 1 of the 3 models is
412 applied on the different herds, or on either morning or evening observations. The RMSEP values for
413 the 3 herds, except for the evening observations of herd C, are very close to each other for the same
414 blood NEFA range (low, middle or high) for either morning or evening observations. This
415 illustrates that the models can be easily transferred to new herds. The RMSEP values for the subsets
416 of evening observations in herd C should be interpreted with caution as each of them is based on a
417 low number of observations ($n \leq 13$, Table 1). Comparing the prediction errors between morning
418 and evening observations for respective subsets shows that the prediction errors for the morning
419 observations are generally higher, especially for blood NEFA concentrations above 0.6 mmol/L
420 (middle and high ranges). For the full model, a one-sided paired *T*-test applied on all the

421 observations of the validation set pointed out that the blood NEFA predictions are more accurate (p
422 = 0.009) if the model is applied on evening milk MIR spectra. This confirms that the blood NEFA
423 concentration in the morning is predicted more accurately from milk MIR spectra taken during the
424 evening milk session of the same day.

425 The observations based on the RMSEP values described in this section are similar to the ones
426 based on the RMSECV values obtained from the cross-validation of the calibration samples (results
427 not shown), confirming the robustness of the models and the validity of this analysis.

428

429 ***Receiver Operating Characteristic Analysis of the Full Model***

430 The smoothed ROC curves for the identification of detrimental blood NEFA concentrations
431 based on the predictions of the full model are shown in Figure 4. Separate smoothed ROC curves
432 are provided for the morning (red) and the evening observations (blue) of the validation set. The
433 AUC of the smoothed ROC curves for the morning and evening observations are respectively 0.860
434 (95% CI: 0.815 – 0.901) and 0.898 (95% CI: 0.860 – 0.930). Accordingly, the AUC for the morning
435 observations is significantly lower ($p < 0.001$) compared to the evening observations. Moreover,
436 compared to the evening observations, the sensitivities for the morning observations are
437 significantly lower in the range of specificities from 0.48 to 0.97. The average sensitivities are
438 0.752 and 0.573 for the morning observations and 0.831 and 0.690 for the evening observations
439 (Figure 4) at specificities of respectively 0.8 and 0.9. Thus, cows with a detrimental blood NEFA
440 concentration, as determined from their morning blood samples, can be detected more accurately
441 using the MIR spectra of their milk collected during the evening milking session of that day.
442 Moreover, it can identify 83 out of 100 cows with detrimental blood NEFA concentrations, while
443 20 out of 100 healthy cows will be wrongly classified as being at risk. Appendix A2 provides the
444 mean values of the sensitivities and the 95% CI of the sensitivities and specificities at given

445 specificities from 0.7 to 0.95 (in steps of 0.05) for the morning and the evening observations of the
446 validation set.

447

448

DISCUSSION

449 *Morning and Evening Milk Samples*

450 The validation of the PLSR models clearly indicates that, compared to morning milk, the MIR
451 spectra of evening milk support more accurate predictions of the NEFA levels in blood taken in the
452 morning of that day (Table 3, Figure 3 and Figure 4). Several studies have shown that blood NEFA
453 follows a diurnal pattern with elevated levels from about 06:00 to 10:00 h in the morning,
454 associated with a reduced energy intake during the night (Blum et al., 2000; Meier et al., 2010;
455 Quiroz-Rocha et al., 2010). For this reason, extra attention was paid to the consistent timing of the
456 blood and milk sampling. As the morning milking session was around 06:30 h, the majority of the
457 period of expected elevated blood NEFA concentrations was after the morning milking session, thus
458 mainly overlapping with the period in which the evening milk was produced. This likely introduced
459 a time delay between the moment of elevated blood NEFA levels and the moment at which a
460 change in the concentration of related milk biomarkers could be noticed, which is even further
461 delayed by the metabolic processes in the liver that transfer NEFA into milk precursors and
462 constituents (e.g. lipoproteins and ketone bodies). this delay would explain why the blood NEFA
463 concentrations were predicted more accurately from MIR spectra of evening milk compared to
464 morning milk as the blood samples were taken within 1 hour after the morning milking session,
465 right in the middle of the time window of expected elevated blood NEFA levels. This hypothesis is
466 also supported by the slightly higher NEFA levels predicted based on MIR spectra of evening milk
467 samples compared to those based on the paired morning milk samples, especially for cows with
468 detrimental blood NEFA concentrations (Figure 3b). It might be interesting for future research to
469 study these dynamics more in detail by measuring the blood NEFA level at a frequent interval and

470 investigating the link with the MIR spectra of morning and evening milk samples on that day and
471 the days after.

472 The fact that the morning blood NEFA concentration can be predicted more accurately when
473 the full model is applied on MIR spectra of evening milk rather than morning milk suggests that the
474 evening milk samples contain more information on the morning blood NEFA concentration and/or
475 that the morning milk samples are more subject to interfering effects. Nevertheless, training the
476 model on solely evening milk MIR spectra (evening model) did not improve the prediction
477 performance compared to the full model, even not if only MIR spectra of evening milk samples are
478 considered in the validation. Moreover, the performance of the evening model was worse if applied
479 on MIR spectra of morning milk samples. This suggests that including morning milk MIR spectra in
480 the calibration set makes the prediction model more robust for potential interfering parameters that
481 vary independent of the cow's blood NEFA level. One of these interfering effects might be the total
482 fat content in the milk, which is generally higher in evening milk compared to morning milk
483 (Forsbäck et al., 2010). Apart from the results obtained in our study, the full model is probably
484 more robust under practical conditions where farms have varying milking and feeding frequencies.

485

486 ***Prediction of Blood Plasma NEFA Concentration***

487 The regression coefficients in Figure 2 show that the PLSR models primarily use information
488 from the fat-related MIR absorption bands. During negative energy status, excessive amounts of
489 NEFA are mobilized from the adipose tissue and part of them is transferred to the milk. These
490 NEFA are particularly rich in long-chain fatty acids (FA), such as C18:1 FA (Jorjong et al., 2014).
491 Dórea et al. (2017) found a nonlinear relation ($R^2 = 0.42$ and $p < 0.001$) between the concentrations
492 of NEFA in the blood plasma and C18:1 FA in the milk fat. Moreover, the milk C18:1 FA increased
493 nearly linearly with increasing blood NEFA for blood NEFA levels below 400 $\mu\text{Eq/L}$, while the
494 milk C18:1 FA concentration was practically constant for blood NEFA concentrations above 800

495 $\mu\text{Eq/L}$. This suggests that the C18:1 FA concentration in milk fat saturates when the blood NEFA
496 increases above a certain concentration. On the other hand, Jorjong et al. (2014) suggested a linear
497 relation ($R^2 = 0.383$) between the concentrations of NEFA in the blood plasma and C18:1 *cis*-9 FA
498 in the milk fat. However, their linear function slightly underestimated the milk C18:1 *cis*-9 FA for
499 blood NEFA concentrations between 0.2 and 0.4 mmol/L, while it overestimated the milk C18:1
500 *cis*-9 FA for blood NEFA levels below 0.1 and above 0.9 mmol/L. Accordingly, the data of Jorjong
501 et al. (2014) confirms the non-linear trend found by Dórea et al. (2017). In our study, the predicted
502 blood NEFA concentrations versus the actual blood NEFA levels (Figure 3b) follows a very similar
503 nonlinear trend as the milk C18:1 FA in the studies of Dórea et al. (2017) and Jorjong et al. (2014).
504 Therefore, it is likely that our PLSR models largely rely on the MIR absorption by C18:1 and
505 related FA in milk. Several researchers already explored MIR spectroscopy to predict the
506 concentration of certain FA in milk, obtaining R^2 values for the prediction of C18:1 FA between
507 0.11 and 0.96 (Rutten et al., 2009; Afseth et al., 2010; Soyeurt et al., 2011). Mäntysaari et al. (2019)
508 used the PLSR models developed by Soyeurt et al. (2011) to predict the milk FA concentrations
509 from milk MIR spectra and accordingly studied the relation between the predicted milk FA and the
510 blood NEFA concentration. It was found that C18:1 *cis*-9 and the sum of C18:1 FA in milk had the
511 highest correlation ($r = 0.73$) with blood NEFA, confirming our hypothesis.

512 The predicted versus measured scatterplot in Figure 3b, as well as the RMSEP values in Table
513 3, clearly show that the accuracy of the prediction of the blood NEFA from milk MIR spectra is
514 limited, especially if the blood NEFA concentration is high. The full model results in RMSEP
515 values of 0.197, 0.182 and 0.190 mmol/L when evaluated on respectively morning observations,
516 evening observations or a mixed set of morning and evening observations of the validation set.
517 Taking into account the standard deviations of the blood NEFA concentration for the different sets
518 (Table 2), the R^2 values are respectively 0.502, 0.613 and 0.558. Nevertheless, the RMSEP and R^2
519 values strongly depend, because of heteroscedasticity, on the proportion of observations with a high

520 blood NEFA concentration in the respective datasets. To account for this non-linear effect, we also
521 explored non-linear models, such as convolutional neural networks, and a logarithmic
522 transformation of the blood NEFA levels before applying PLSR without success. Moreover, using a
523 more balanced calibration set with a similar number of observations with high and low blood NEFA
524 levels through bootstrapping did not improve the performance of the prediction model either
525 (results not shown). Because of the heteroscedasticity of the prediction error, benchmarking our
526 results against earlier studies is challenging and should be done with caution.

527 Dórea et al. (2017) obtained RMSE values of 169 – 220 $\mu\text{Eq/L}$ (equivalent to $\mu\text{mol/L}$) and R^2
528 values of 0.080 – 0.457 for the prediction of blood NEFA levels for individual cows from different
529 linear combinations or ratios of milk FA concentrations obtained from GLS analysis. As the
530 descriptive statistics for the blood NEFA are very similar in their dataset and ours (Table 2), it is
531 fair to compare the results of these 2 studies. The prediction errors reported by Dórea et al. are very
532 close to the ones obtained in our study. Nevertheless, the performances of their models are only
533 reported for the calibration set and thus might be overoptimistic. Additionally, the approach
534 followed by Dórea et al. requires labor and cost intensive FA isolation and GLS analysis.

535 Mäntysaari et al. (2019) used a linear combination of C18:1 *cis*-9 and medium chain FA
536 concentrations in milk, derived from evening milk MIR spectra, and lactation stage to predict the
537 morning blood NEFA concentration, obtaining an R^2 of 0.61 and an RMSECV of 0.182 mmol/L. A
538 similar approach using morning milk MIR spectra resulted in an R^2 of 0.52 and an RMSECV of
539 0.198 mmol/L. Although these results only represent the cross-validation of the model, and thus
540 might be overoptimistic, they are in close agreement with the results obtained for the independent
541 validation in our study.

542 Recently, Benedet et al. (2019), Grelet et al. (2019) and Luke et al. (2019) published PLSR
543 models that predict the blood NEFA levels directly from the MIR spectra of raw milk samples. The
544 prediction performance of Grelet's model ($R^2 = 0.39$ and RMSECV = 344 $\mu\text{eq/L}$) is only based on

545 cross-validation of the calibration set and should thus be confirmed on an external validation set
546 (Grelet et al., 2019). Still, their results are inferior to the ones obtained in our study due to the
547 higher prediction error by Grelet's model in the low blood NEFA range. Moreover, while our full
548 model is relatively accurate ($RMSEP \leq 0.143$ mmol/L) in this range, Grelet's model generally
549 overestimates the low blood NEFA concentrations. In the high blood NEFA range, Grelet's model
550 performs similar to our models, both underestimating the blood NEFA concentration. As a result,
551 the prediction error of Grelet's model is nearly homoscedastic, but worse compared to our model,
552 especially in the low blood NEFA range. Benedet et al. (2019) obtained a PLSR model that
553 performed better, compared to Grelet's model, with an R^2 of 0.52 and a standard error of prediction
554 $\left[SEP = n\sqrt{RMSEP^2 - bias^2}/(n - 1) \right]$ of 0.24 mmol/L for a randomly selected validation set.
555 Still, these results are slightly worse compared to the ones obtained in our study. In contrast to our
556 models, Benedet's model only uses wavenumbers between 1450 and 1000 cm^{-1} and thus ignores the
557 fat absorption bands at around 2928, 2858 and 1745 cm^{-1} . Additionally, it should be taken into
558 account that the model performance typically deteriorates when it is applied on a completely
559 independent herd, as illustrated by Luke et al. (2019). Moreover, the R^2 of Luke's model dropped
560 from 0.61 for a randomly selected validation set, covering the same herds as the calibration set, to
561 0.45 for a totally independent herd. The better performance of our full model is likely the result of a
562 higher number of calibration samples ($n = 790$) in combination with a well-controlled timing and
563 protocol for blood and milk sample collection (Quiroz-Rocha et al., 2010).

564

565 ***Receiver Operating Characteristic Analysis***

566 Unlike the regression analysis, in which the RMSE is subject to the effect of heteroscedasticity,
567 the result of the ROC analysis is less dependent on the relative number of observations with a high
568 blood NEFA concentration. Accordingly, these ROC analyses allow for a more objective
569 comparison among different studies. Dórea et al. (2017) obtained their best results to identify cows

570 with detrimental blood NEFA concentrations ($\geq 600 \mu\text{Eq/L}$) based on the milk C13:0 FA using a
571 threshold of 0.036 g FA per 100 g milk fat. This resulted in an AUC, sensitivity and specificity of
572 respectively 0.90, 0.859 and 0.823. The ROC curve to detect detrimental blood NEFA levels based
573 on milk C18:1 *cis*-9 FA and reported by Jorjong et al. (2014) had a sensitivity of 0.75 and 0.5 at a
574 specificity of respectively 0.79 and 0.935. The full model obtained in our approach and applied on
575 the evening observations results in an AUC of 0.898 and a sensitivity of 0.831 at a specificity of
576 0.8. The same model applied on morning observations has an AUC of 0.860 and a sensitivity of
577 0.752 at a specificity of 0.8 (Appendix A2). Therefore, it can be concluded that our model, which
578 only requires MIR spectral analysis of raw milk, is not inferior compared to more complex
579 techniques that require characterization of certain FA in the milk fat. A similar approach followed
580 by Luke et al. (2019) to identify elevated blood NEFA levels resulted in a AUC values of 0.87 and
581 0.82, sensitivities of 0.73 and 0.25 and specificities of 0.81 and 0.90 for respectively a randomly
582 selected and a completely independent validation set. Thus, our model tends to be slight more
583 robust compared to the one of Luke et al. (2019).

584 Although the prediction accuracy is not excellent, the developed model can provide valuable
585 information to further improve genetics, nutrition and management of dairy cows. As it can be
586 applied on millions of historical and future milk MIR spectra, this approach can reveal detailed
587 information on the energy status of individual cows, herds and pedigrees. This could potentially
588 result in improved estimations of breeding values and the identification of specific genetic markers
589 for metabolic resilience.

590

591

CONCLUSIONS

592 In this study, we successfully predicted the blood NEFA level in individual dairy cows from
593 their milk MIR spectra. The best model was obtained after training on MIR spectra of both morning
594 and evening milk samples. The NEFA concentration of blood plasma samples taken in the morning

595 were predicted with a higher accuracy if the model was applied on MIR spectra of evening milk
596 samples. The obtained prediction accuracy is acceptable for low blood NEFA levels, but is
597 unsatisfactory if the blood NEFA concentration is high. Nevertheless, low and intermediate/high
598 blood NEFA levels could be discriminated well to identify 83 out of 100 cows with detrimental
599 blood NEFA levels, while only 20 out of 100 healthy cows are wrongly classified. This opens
600 opportunities for identifying cows at risk of a negative energy status and studying the metabolic
601 resilience of individual cows and pedigrees.

602

603

ACKNOWLEDGEMENTS

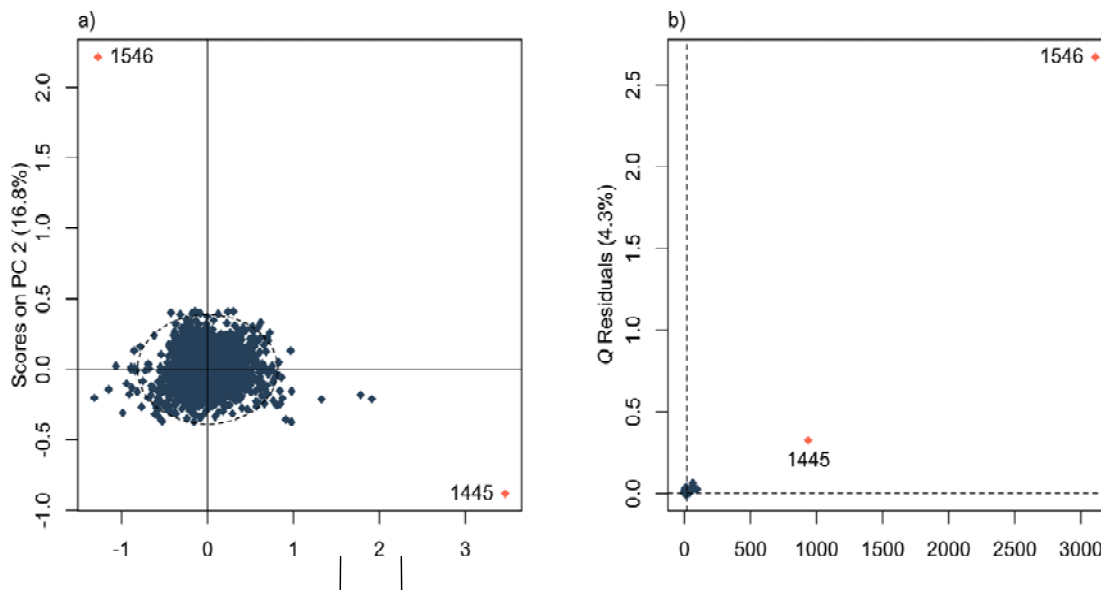
604 This study was funded by the Finnish Ministry of Agriculture and Forestry (1844/312/2012),
605 Valio Ltd, Faba co-op, Viking Genetics, Finnish Cattle Breeding Foundation and Raisioagro Ltd.
606 Ben Aernouts and Ines Adriaens were respectively funded as postdoctoral fellow (11ZG916N) and
607 aspirant fellow (12K3916N) by the Research Foundation Flanders (FWO, Brussels, Belgium). Ben
608 Aernouts obtained additional funding from the Research Foundation Flanders to perform a long
609 research stay abroad at the Natural Resources Institute of Finland (Luke), grant V407018N.

610

APPENDICES

611 **Appendix A1** Figures of a) The scores plot of principal component (PC) 1 versus PC2 of the
612 principal component analysis (PCA) on all 1585 mean-centered mid-infrared transmittance spectra.
613 The dashed ellipse represents the 99% confidence limits of the scores on PC1 and PC2. b) The
614 influence plot (Q residual versus Hotelling T^2 statistics) for the PCA model with 7 PC presenting
615 the of the PCA. The dashed lines represent the 99% confidence limits on respectively the 2
616 statistics. In both figures, each dot represents a different sample spectrum and the red dots (with
617 sample number) indicate potential outlier spectra.

618



619 **Appendix A2** Table with the mean values of the sensitivities and the 95% confidence intervals (CI)
620 of the sensitivities and specificities at given specificities for the morning and the evening
621 observations of the validation set.

622

Sp	Morning observations			Evening observations		
	95% CI Sp	Se	95% CI Se	95% CI Sp	Se	95% CI Se
0.700	0.600 - 0.794	0.850	0.775 - 0.924	0.584 - 0.800	0.902	0.841 - 0.953
0.750	0.661 - 0.830	0.807	0.725 - 0.890	0.648 - 0.835	0.872	0.803 - 0.932
0.800	0.724 - 0.866	0.752	0.661 - 0.844	0.714 - 0.870	0.831	0.754 - 0.902
0.850	0.788 - 0.902	0.678	0.577 - 0.778	0.781 - 0.905	0.775	0.687 - 0.856
0.900	0.852 - 0.939	0.573	0.463 - 0.683	0.848 - 0.941	0.690	0.589 - 0.785
0.950	0.918 - 0.974	0.410	0.293 - 0.533	0.916 - 0.974	0.545	0.425 - 0.660

Sp = specificity; Se = sensitivity

623

REFERENCES

624

Adewuyi, A.A., E. Gruysi, and F.J.C.M.V. Eerdenburg. 2005. Non esterified fatty acids

625

(NEFA) in dairy cattle. A review. *Vet. Q.* 27:117–126. doi:10.1080/01652176.2005.9695192.

626

Aernouts, B., E. Polshin, W. Saeys, and J. Lammertyn. 2011. Mid-infrared spectrometry of

627

milk for dairy metabolomics: a comparison of two sampling techniques and effect of

628

homogenization. *Anal. Chim. Acta* 705:88–97. doi:10.1016/j.aca.2011.04.018.

629

Afseth, N.K., H. Martens, Å. Randby, L. Gidskehaug, B. Narum, K. Jørgensen, S. Lien, and A.

630

Kohler. 2010. Predicting the fatty acid composition of milk: A comparison of two fourier transform

631

infrared sampling techniques. *Appl. Spectrosc.* 64:700–707. doi:10.1366/000370210791666200.

632

Barnes, R.J., M.S. Dhanoa, and S.J. Lister. 1989. Standard normal variate transformation and

633

de-trending of near-infrared diffuse reflectance spectra. *Appl. Spectrosc.* 43:772–777.

634

doi:10.1366/0003702894202201.

635

Beer. 1852. Bestimmung der Absorption des rothen Lichts in farbigen Flüssigkeiten. *Ann.*

636

Phys. 162:78–88. doi:10.1002/andp.18521620505.

637

Benedet, A., M. Franzoi, M. Penasa, E. Pellattiero, and M. De Marchi. 2019. Prediction of

638

blood metabolites from milk mid-infrared spectra in early-lactation cows. *J. Dairy Sci.*

639

doi:10.3168/jds.2019-16937.

640

Bjerre-Harpøth, V., N.C. Friggens, V.M. Thorup, T. Larsen, B.M. Damgaard, K.L. Ingvarsten,

641

and K.M. Moyes. 2012. Metabolic and production profiles of dairy cows in response to decreased

642

nutrient density to increase physiological imbalance at different stages of lactation. *J. Dairy Sci.*

643

95:2362–2380. doi:10.3168/jds.2011-4419.

644

Blum, J.W., R.M. Bruckmaier, P.Y. Vacher, A. Münger, and F. Jans. 2000. Twenty-Four-Hour

645

Patterns of Hormones and Metabolites in Week 9 and 19 of Lactation in High-Yielding Dairy Cows

646

fed Triglycerides and Free Fatty Acids. *J. Vet. Med. Ser. A Physiol. Pathol. Clin. Med.* 47:43–60.

647

doi:10.1046/j.1439-0442.2000.00266.x.

- 648 Bro, R., and A.K. Smilde. 2014. Principal component analysis. *Anal. Methods* 6:2812–2831.
649 doi:10.1039/c3ay41907j.
- 650 Cederkvist, H.R., A.H. Aastveit, and T. Næs. 2005. A comparison of methods for testing
651 differences in predictive ability. *J. Chemom.* 19:500–509. doi:10.1002/cem.956.
- 652 Chong, I.G., and C.H. Jun. 2005. Performance of some variable selection methods when
653 multicollinearity is present. *Chemom. Intell. Lab. Syst.* 78:103–112.
654 doi:10.1016/j.chemolab.2004.12.011.
- 655 Dórea, J.R.R., E.A. French, and L.E. Armentano. 2017. Use of milk fatty acids to estimate
656 plasma nonesterified fatty acid concentrations as an indicator of animal energy balance. *J. Dairy
657 Sci.* 100:6164–6176. doi:10.3168/jds.2016-12466.
- 658 Enjalbert, F., M.C. Nicot, C. Bayourthe, and R. Moncoulon. 2010. Ketone Bodies in Milk and
659 Blood of Dairy Cows: Relationship between Concentrations and Utilization for Detection of
660 Subclinical Ketosis. *J. Dairy Sci.* 84:583–589. doi:10.3168/jds.s0022-0302(01)74511-0.
- 661 Fawcett, T. 2006. An Introduction to ROC analysis. *Pattern Recognit. Lett.* 27:861–874.
662 doi:10.1016/j.patrec.2005.10.010.
- 663 Forsbäck, L., H. Lindmark-Månsson, A. Andrén, M. Akerstedt, L. Andrée, and K. Svennersten-
664 Sjaunja. 2010. Day-to-day variation in milk yield and milk composition at the udder-quarter level. *J.
665 Dairy Sci.* 93:3569–3577. doi:10.3168/jds.2009-3015.
- 666 Fox, P.F., and P.L.H. McSweeney. 2006. *Advanced Dairy Chemistry Volume 2: Lipids*. 3rd ed.
667 Springer, New York, USA.
- 668 Franzoi, M., G. Niero, G. Visentin, M. Penasa, M. Cassandro, and M. De Marchi. 2019.
669 Variation of Detailed Protein Composition of Cow Milk Predicted from a Large Database of Mid-
670 Infrared Spectra. *Animals* 9:176. doi:10.3390/ani9040176.

- 671 Geladi, P., D. MacDougall, and H. Martens. 1985. Linearization and Scatter-Correction for
672 Near-Infrared Reflectance Spectra of Meat. *Appl. Spectrosc.* 39:491–500.
673 doi:10.1366/0003702854248656.
- 674 Grelet, C., C. Bastin, M. Gelé, J.-B. Davière, M. Johan, A. Werner, R. Reding, J.A. Fernandez
675 Pierna, F.G. Colinet, P. Dardenne, N. Gengler, H. Soyeurt, and F. Dehareng. 2016. Development of
676 Fourier transform mid-infrared calibrations to predict acetone, β -hydroxybutyrate, and citrate
677 contents in bovine milk through a European dairy network. *J. Dairy Sci.* 99:4816–4825.
678 doi:10.3168/jds.2015-10477.
- 679 Grelet, C., J.A. Fernández Pierna, P. Dardenne, V. Baeten, and F. Dehareng. 2015.
680 Standardization of milk mid-infrared spectra from a European dairy network. *J. Dairy Sci.* 98:2150–
681 2160. doi:10.3168/jds.2014-8764.
- 682 Grelet, C., A. Vanlierde, M. Hostens, L. Foldager, M. Salavati, K.L. Ingvarsen, M. Crowe,
683 M.T. Sorensen, E. Froidmont, C.P. Ferris, C. Marchitelli, F. Becker, T. Larsen, F. Carter, and F.
684 Dehareng. 2019. Potential of milk mid-IR spectra to predict metabolic status of cows through blood
685 components and an innovative clustering approach. *Animal* 13:649–658.
686 doi:10.1017/S1751731118001751.
- 687 Van Haelst, Y.N.T., A. Beeckman, A.T.M. Van Kneghsel, and V. Fievez. 2008. Short
688 Communication: Elevated Concentrations of Oleic Acid and Long-Chain Fatty Acids in Milk Fat of
689 Multiparous Subclinical Ketotic Cows. *J. Dairy Sci.* 91:4683–4686. doi:10.3168/jds.2008-1375.
- 690 ICAR. 2019. Section 12 - Guidelines for Milk Analysis.
- 691 ISO. 2013. Milk and liquid milk products -- Guidelines for the application of mid-infrared
692 spectrometry. Page 14 in International Standard ISO 9622:2013/IDF 141:2013. International Dairy
693 Federation.
- 694 Jorjong, S., A.T.M. van Kneghsel, J. Verwaeren, M.V. Lahoz, R.M. Bruckmaier, B. De Baets, B.
695 Kemp, and V. Fievez. 2014. Milk fatty acids as possible biomarkers to early diagnose elevated

696 concentrations of blood plasma nonesterified fatty acids in dairy cows. *J. Dairy Sci.* 97:7054–7064.
697 doi:10.3168/jds.2014-8039.

698 Kemp, B.J., W. Saeys, K. Mertens, P. Darius, J.G. De Baerdemaeker, and B. De Ketelaere.
699 2010. The importance of choosing the right validation strategy in inverse modelling. *J. Near*
700 *Infrared Spectrosc.* 18:231–237. doi:10.1255/jnirs.882.

701 Leblanc, S. 2010. Monitoring Metabolic Health of Dairy Cattle in the Transition Period. *J.*
702 *Reprod. Dev.* 56:S29–S35. doi:10.1262/jrd.1056S29.

703 Leroy, J.L.M.R., P. Bossaert, G. Opsomer, and P.E.J. Bols. 2011. The effect of animal handling
704 procedures on the blood non-esterified fatty acid and glucose concentrations of lactating dairy cows.
705 *Vet. J.* 187:81–84. doi:10.1016/j.tvjl.2009.10.003.

706 Leroy, J.L.M.R., T. Vanholder, B. Mateusen, A. Christophe, G. Opsomer, A. de Kruif, G.
707 Genicot, and A. Van Soom. 2005. Non-esterified fatty acids in follicular fluid of dairy cows and
708 their effect on developmental capacity of bovine oocytes in vitro. *Reproduction* 130:485–495.
709 doi:10.1530/rep.1.00735.

710 Luke, T.D., S. Rochfort, W.J. Wales, V. Bonfatti, L. Marett, and J.E. Pryce. 2019. Metabolic
711 profiling of early-lactation dairy cows using milk mid-infrared spectra. *J. Dairy Sci.* 102:1747–
712 1760. doi:10.3168/jds.2018-15103.

713 Mäntysaari, P., E.A. Mäntysaari, T. Kokkonen, T. Mehtiö, S. Kajava, C. Grelet, P. Lidauer, and
714 M.H. Lidauer. 2019. Body and milk traits as indicators of dairy cow energy status in early lactation.
715 *J. Dairy Sci.* 102:7904–7916. doi:10.3168/jds.2018-15792.

716 De Marchi, M., C.C. Fagan, C.P. O’Donnell, A. Cecchinato, R. Dal Zotto, M. Cassandro, M.
717 Penasa, and G. Bittante. 2009. Prediction of coagulation properties, titratable acidity, and pH of
718 bovine milk using mid-infrared spectroscopy. *J. Dairy Sci.* 92:423–432. doi:10.3168/jds.2008-1163.

- 719 De Marchi, M., V. Toffanin, M. Cassandro, and M. Penasa. 2014. Invited review: Mid-infrared
720 spectroscopy as phenotyping tool for milk traits I. *J. Dairy Sci.* 97:1171–1186.
721 doi:10.3168/jds.2013-6799.
- 722 Martens, H., and T. Næs. 1987. *Multivariate calibration by data compression*. P.C. Williams
723 and K. Norris, ed. American Association of Cereal Chemists, St Paul, MN, USA.
- 724 Meier, S., E.S. Kolver, G.A. Verkerk, and J.R. Roche. 2010. Effects of divergent Holstein-
725 Friesian strain and diet on diurnal patterns of plasma metabolites and hormones. *J. Dairy Res.*
726 77:432–437. doi:10.1017/S002202991000052X.
- 727 Norgaard, L., J. Wagner, J.P. Nielsen, L. Munc, and S.B. Engelsen. 2000. Interval Partial
728 Least-Squares Regression (iPLS): A comparative chemometric study with an example from Near-
729 Infrared Spectroscopy. *Appl. Spectrosc.* 54:413–419. doi:10.1366/0003702001949500.
- 730 Ospina, P.A., D.V. Nydam, T. Stokol, and T.R. Overton. 2010a. Associations of elevated
731 nonesterified fatty acids and β -hydroxybutyrate concentrations with early lactation reproductive
732 performance and milk production in transition dairy cattle in the northeastern United States. *J. Dairy*
733 *Sci.* 93:1596–1603. doi:10.3168/jds.2009-2852.
- 734 Ospina, P.A., D.V. Nydam, T. Stokol, and T.R. Overton. 2010b. Evaluation of nonesterified
735 fatty acids and β -hydroxybutyrate in transition dairy cattle in the northeastern United States: Critical
736 thresholds for prediction of clinical diseases. *J. Dairy Sci.* 93:546–554. doi:10.3168/jds.2009-2277.
- 737 Quiroz-Rocha, G.F., S.J. LeBlanc, T.F. Duffield, B. Jefferson, D. Wood, K.E. Leslie, and R.M.
738 Jacobs. 2010. Short communication: Effect of sampling time relative to the first daily feeding on
739 interpretation of serum fatty acid and β -hydroxybutyrate concentrations in dairy cattle. *J. Dairy Sci.*
740 93:2030–2033. doi:10.3168/jds.2009-2141.
- 741 R Core Team. 2017. *R: A language and environment for statistical computing*. Vienna, Austria.

- 742 Robin, X., N. Turck, A. Hainard, N. Tiberti, F. Lisacek, J. Sanchez, and M. Müller. 2011.
743 pROC: an open-source package for R and S+ to analyze and compare ROC curves. *BMC*
744 *Bioinformatics* 12:1–8.
- 745 Ruckstuhl, A.F., M.P. Jacobson, R.W. Field, and J.A. Dodd. 2001. Baseline subtraction using
746 robust local regression estimation. *J. Quant. Spectrosc. Radiat. Transf.* 68:179–193.
747 doi:10.1016/S0022-4073(00)00021-2.
- 748 Rutten, M.J.M., H. Bovenhuis, K.A. Hettinga, H.J.F. van Valenberg, and J.A.M. van Arendonk.
749 2009. Predicting bovine milk fat composition using infrared spectroscopy based on milk samples
750 collected in winter and summer. *J. Dairy Sci.* 92:6202–6209. doi:10.3168/jds.2009-2456.
- 751 Salin, S., J. Taponen, K. Elo, I. Simpura, A. Vanhatalo, R. Boston, and T. Kokkonen. 2012.
752 Effects of abomasal infusion of tallow or camelina oil on responses to glucose and insulin in dairy
753 cows during late pregnancy. *J. Dairy Sci.* 95:3812–25. doi:10.3168/jds.2011-5206.
- 754 Savitzky, A., and M.J.E. Golay. 1964. Smoothing and Differentiation of Data by Simplified
755 Least Squares Procedures. *Anal. Chem.* 36:1627–1639. doi:10.1021/ac60214a047.
- 756 Scalia, D., N. Lacetera, U. Bernabucci, K. Demeyere, L. Duchateau, and C. Burvenich. 2006.
757 In Vitro Effects of Nonesterified Fatty Acids on Bovine Neutrophils Oxidative Burst and Viability.
758 *J. Dairy Sci.* 89:147–154. doi:10.3168/jds.s0022-0302(06)72078-1.
- 759 Snee, R. 1977. Validation of regression models: methods and examples. *Technometrics*
760 19:415–428. doi:10.2307/1267881.
- 761 Soyeur, H., D. Bruwier, J.-M. Romnee, N. Gengler, C. Bertozzi, D. Veselko, and P. Dardenne.
762 2009. Potential estimation of major mineral contents in cow milk using mid-infrared spectrometry.
763 *J. Dairy Sci.* 92:2444–2454. doi:10.3168/jds.2008-1734.
- 764 Soyeur, H., F. Dehareng, N. Gengler, S. Mcparland, E. Wall, D.P. Berry, and M. Coffey. 2011.
765 Mid-infrared prediction of bovine milk fatty acids across multiple breeds, production systems, and
766 countries. *J. Dairy Sci.* 94:1657–1667. doi:10.3168/jds.2010-3408.

767 Westad, F., and H. Martens. 2000. Variable selection in near infrared spectroscopy based on
768 significance testing in partial least squares regression. *J. Near Infrared Spectrosc.* 8:117–124.
769 doi:10.1255/jnirs.271.

770 Williams, P., and K. Norris. 2001. *Near-Infrared Technology in the Agricultural and Food*
771 *Industries*. 2nd ed. American Association of Cereal Chemist, St. Paul, USA.

772

773

TABLES

774 **Table 1** Number of mid-infrared (MIR) transmittance spectra of morning and evening milk samples

775 available for the 3 different herds included in this study.

Milk samples	All herds	Herd		
		A	B	C
Morning	808	640	121	47
Evening	777	646	118	13

776 **Table 2** The descriptive statistics of the blood plasma non-esterified fatty acid (NEFA) concentrations linked to different subsets of milk mid-
 777 infrared transmittance spectra.

Blood NEFA (mmol/L)	Calibration set (Herd A)			Validation set (Herd A, B and C)								
	Overall	Morning	Evening	Overall	Morning samples				Evening samples			
					All herds	Herd A	Herd B	Herd C	All herds	Herd A	Herd B	Herd C
Number	790	395	395	793	412	245	121	46	381	251	117	13
Mean	0.436	0.436	0.435	0.445	0.442	0.477	0.372	0.444	0.448	0.479	0.372	0.530
SD	0.296	0.296	0.296	0.286	0.280	0.316	0.187	0.246	0.292	0.324	0.188	0.298
Minimum	0.036	0.036	0.036	0.055	0.055	0.055	0.069	0.087	0.055	0.055	0.069	0.092
Maximum	1.951	1.951	1.951	1.748	1.631	1.631	1.080	1.256	1.748	1.748	1.080	1.033

778 **Table 3** Root mean squared error of prediction (RMSEP) for the non-esterified fatty acid (NEFA) concentration in the blood plasma by the
779 partial least squares regression models trained on morning and evening observations (= full model), only morning observations (= morning
780 model) and only evening observations (= evening model) of the calibration set. The RMSEP values are provided for the different subsets (blood
781 NEFA range, milking time and herd) of the validation set. Within each column and a specified blood NEFA concentration range, the RMSEP
782 values with different subscripts indicate significant ($\alpha = 0.05$) differences between the models according to Tukey HSD multiple comparison,
783 with a letter lower in the alphabetical order indicating a better model.

Blood NEFA range (mmol/L)	Model	Validation set - RMSEP (mmol/L)								
		Overall	Morning observations				Evening observations			
			All herds	Herd A	Herd B	Herd C	All herds	Herd A	Herd B	Herd C
Complete: 0 – 2	Full	0.190 ^a	0.197 ^a	0.220 ^a	0.135	0.204	0.182 ^a	0.199 ^a	0.140 ^a	0.167
	Morning	0.194 ^b	0.194 ^a	0.211 ^a	0.143	0.209	0.194 ^b	0.207 ^b	0.169 ^b	0.139
	Evening	0.206 ^b	0.225 ^b	0.252 ^b	0.161	0.220	0.183 ^a	0.195 ^a	0.156 ^{a,b}	0.162
Low: 0 – 0.6	Full	0.129 ^a	0.124 ^a	0.132	0.109	0.128	0.134 ^a	0.143 ^b	0.122 ^a	0.062
	Morning	0.158 ^b	0.141 ^b	0.145	0.129	0.152	0.174 ^b	0.184 ^c	0.161 ^b	0.071
	Evening	0.132 ^a	0.136 ^{a,b}	0.135	0.135	0.145	0.128 ^a	0.120 ^a	0.143 ^a	0.098
Middle: 0.6 – 1.2	Full	0.241 ^b	0.269 ^b	0.270 ^b	0.253 ^{a,b}	0.290 ^{a,b}	0.208 ^{a,b}	0.198 ^{a,b}	0.230	0.258
	Morning	0.211 ^a	0.234 ^a	0.232 ^a	0.218 ^a	0.277 ^a	0.185 ^a	0.174 ^a	0.219	0.206
	Evening	0.281 ^c	0.328 ^c	0.339 ^c	0.286 ^b	0.322 ^b	0.223 ^b	0.221 ^b	0.226	0.231
High: 1.2 – 2	Full	0.668 ^b	0.713 ^b	0.704 ^b		0.793	0.620 ^b	0.620 ^b		
	Morning	0.607 ^a	0.675 ^a	0.668 ^a		0.738	0.530 ^a	0.530 ^a		
	Evening	0.711 ^c	0.781 ^c	0.780 ^c		0.784	0.633 ^b	0.633 ^b		

784

FIGURES

785 **Figure 1** Schematic overview of the methodology to build a partial least squares (PLSR) model to
786 predict the blood plasma non-esterified fatty acid concentration from milk mid-infrared spectra. CV
787 = cross-validation, RMSECV = root mean square error of cross-validation, RMSEP = root mean
788 square error of prediction.

789

790 **Figure 2** Top: Relative mid-infrared (MIR) transmittance spectra of the milk samples. The dotted
791 black lines (with sample number) indicate 2 potential outlier spectra. The grey regions indicate the
792 wavenumbers included in at least 1 of the 3 final partial least squares regression (PLSR) models
793 (full, morning or evening) to predict the blood plasma non-esterified fatty acid concentration after
794 applying a variable selection technique. Bottom: Regression coefficients for the 3 different PLSR
795 models constructed using a calibration set with MIR spectra of respectively i) morning and evening
796 milk samples (= full model, green solid), ii) only morning milk samples (= morning model, red
797 dashed) and iii) only evening milk samples (= evening model, blue dotted) of herd A.

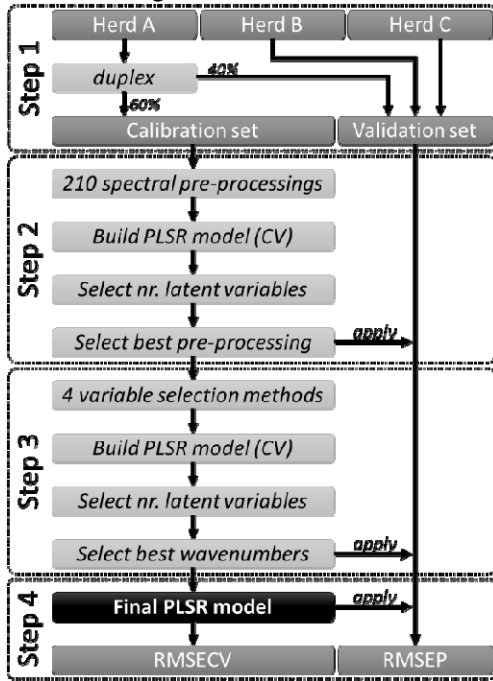
798

799 **Figure 3** The results of the partial least squares regression (PLSR) model trained on a calibration
800 set of mid-infrared transmittance spectra of milk samples collected during morning and evening
801 milking sessions (= full model) on herd A to predict the non-esterified fatty acid (NEFA)
802 concentration in the blood plasma of the respective cows for which blood was sampled in the
803 morning. a) Root mean squared error (RMSE) for the calibration set in cross-validation (CV) and
804 the morning (P_M) and evening (P_E) observations of the validation set (all 3 herds), in relation to the
805 number of latent variables of the PLSR model. The green triangle indicates the number of selected
806 latent variables ($n = 6$) for the final PLSR model. b) The predicted versus measured scatterplot for
807 the calibration set (herd A) in cross-validation (CV) and the morning (P_M) and evening (P_E)
808 observations of the validation set (3 herds).

809

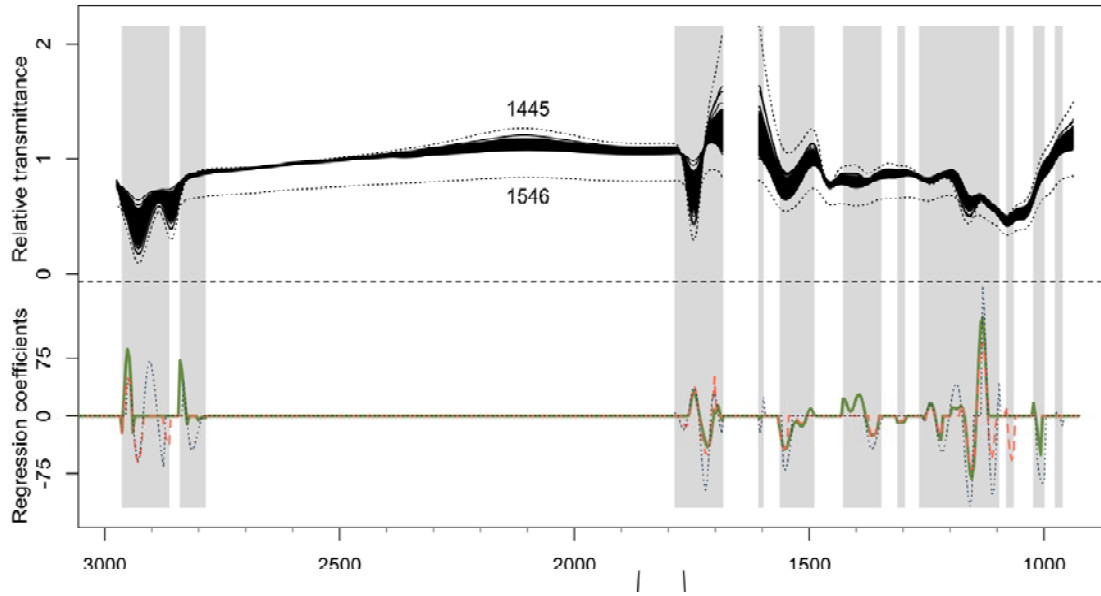
810 **Figure 4** Smoothed receiver operating characteristic (ROC) curves for the identification of
811 detrimental blood plasma non-esterified fatty acid (NEFA) concentrations (≥ 0.6 mmol/L). The
812 NEFA concentrations were predicted with partial least squares regression models trained on
813 morning and evening observations (= full model) of the calibration set. The mean values (lines) and
814 95% confidence intervals (areas) for the smoothed ROC curves are provided for morning (red,
815 dashed) and evening observations (blue, dotted) of the validation set.

816 Aernouts, Figure 1



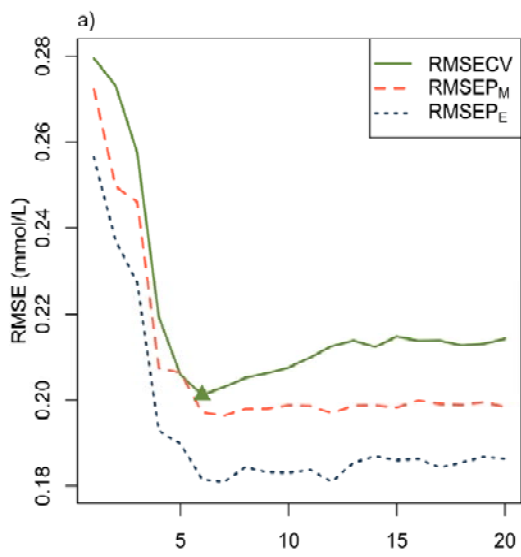
817

818 Aernouts, Figure 2

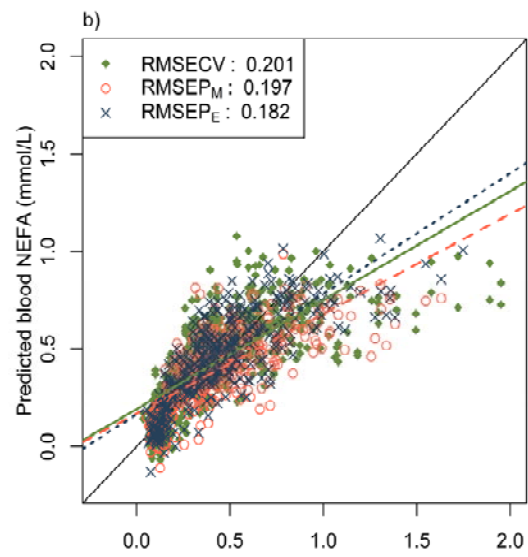


819

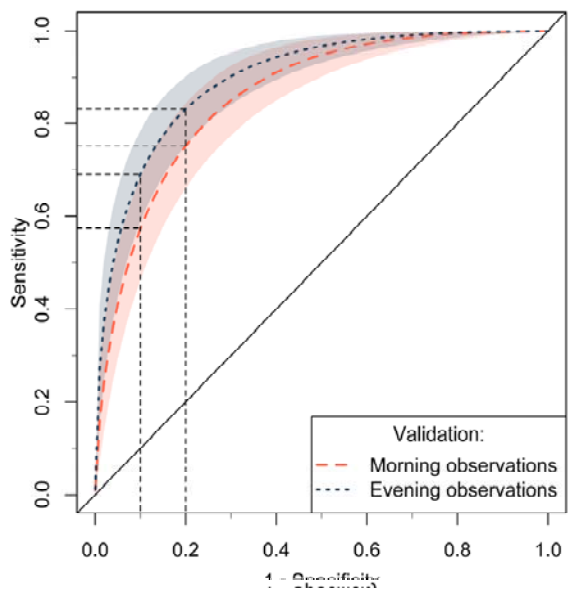
820 Aernouts, Figure 3



821



822 Aernouts, Figure 4



823